Jurnal Tribologi 47 (2025) 171-182

MYTRIBOS Malaysian Tribology Society

Jurnal Tribologi

Website : jurnaltribologi.mytribos.org e-issn: 2289-7232

Multiaxial compression of stainless steel 304 and its wear behavior

Aditya K. Padap *, Raeeshul H. Ansari, Narendra Kumar

Mechanical Engineering Department, Bundelkhand Institute of Engineering and Technology Jhansi, UP, 284128 INDIA.
*Corresponding author: padap@rediffmail.com

KEYWORDS

Severe plastic deformation
Multi-axial compression
Grain refinement
Wear
Tribology
Pin on disc

ABSTRACT

This study aims to develop the high strength stainless steel for biomedical application by multiaxial compression (MAC) technique. MAC is a severe plastic deformation (SPD) technique having significant potential for producing refined grains. Further, the impact of grain refinement on wear behavior is also studied. Vicker's Hardness of six MAC pass sample was observed about 2.3 times greater compared to annealed sample. Increased hardness is attributed to strain hardening. High hardness might be responsible for high wear resistance according to Archard's wear law. But few study shows the reverse trend of wear resistance due to some other parameters e.g. humidity brittleness and fragmentation of other phases into the matrix. Hence wear study was carried out for investigating the interesting wear behavior. At room temperature, tribological characteristics were corelated with micro structural modifications of MAC processed stainless steel. The results were verified using scanning electron microscope (SEM) analysis of wear pin. Under the SEM, worn surfaces were analyzed for identifying the wear mechanism.

1.0 INTRODUCTION

Traditionally, steels have been widely utilized due to their high strength, corrosion resistance, and good wear properties (Callister & Rethwisch, 2014). However, modern structural applications demand materials that combine high strength with superior toughness, enhanced formability, excellent weldability, and cost-effectiveness (Padap et al., 2009, Bhadeshia & Honeycombe, 2017). These multifunctional requirements can be effectively addressed through

Received 28 July 2025; received in revised form 16 September 2025; accepted 6 October 2025.
To cite this article: Padap et al. (2025). Multiaxial compression of stainless steel 304 and its wear behavior. Jurnal Tribologi 47, pp.171-182.

grain refinement techniques, particularly by employing Severe Plastic Deformation (SPD) processes (Valiev et al., 2000, Zhilyaev & Langdon, 2008). Among SPD techniques, the development of ultrafine-grained (UFG) steels via Multiaxial Compression (MAC) offers a comparatively simple and economically viable route, especially when compared to producing high-strength low-alloy (HSLA) steels or metal matrix nanocomposites (Ma, 2003, Padap et al., 2010). Accumulative Roll Bonding (ARB) processed Aluminum Alloy demonstrate mechanical properties comparable to, or exceeding, those of conventionally alloyed steels, making them promising candidates for structural applications (Tsuji et al., 2002).

Multiaxial Compression (MAC) has been extensively employed by researchers for the development of UFG materials due to its capability to impose large plastic strains through complex strain paths (Valiev et al., 1999, Han & Xu, 2006). In particular, for composite materials and steels with ferrite–pearlite microstructures (such as mild steel), MAC-induced deformation significantly influences microstructural evolution by altering phase morphology and refining grain structure (Aravindh et al., 2025, Meyers & Chawla, 2008). The application of multiaxial strain paths and high deformation rates during other SPD techniques like Accumulative roll bonding (ARB) and high-pressure torsion (HPT) facilitates enhanced grain refinement and dislocation activity compared to conventional methods (Tsuji et al., 1999, Xu et al., 2007). One of the primary advantages of UFG steels lies in their ability to achieve high strength without the need for additional alloying elements or complex post-processing steps, such as annealing, quenching, or tempering (Sauvage et al., 2008, Vinogradov & Hashimoto, 2001). This makes SPD-processed steels not only structurally robust but also cost-efficient and environmentally sustainable.

According to Archard's Wear law, the change in mechanical properties viz hardness, tensile strength due to SPD would also affect the wear characteristics of UFG materials. A simplified yet practical definition characterizes wear as damage to a solid surface, often involving gradual material removal due to mechanical interaction with another material in motion (Bhushan, 2013). Wear, whether mechanical, chemical, or synergistic, is one of the primary causes of surface degradation in engineering components and often operates alongside other failure mechanisms such as fatigue, creep, and corrosion (Rabinowicz, 2013). The complex nature of wear arises from multiple interacting parameters—material properties, environment, surface conditions, loading, lubrication, and contact mechanics—all of which evolve during service (Blau, 2001). Consequently, predicting wear remains a challenge for tribologists and design engineers due to these dynamically changing interfacial conditions (Suh, 1973).

Research on UFG ferrous materials has shown significant advancements in their mechanical properties. Song et al. (2005) found that 0.2% C-Mn UFG steel exhibited enhanced strength and toughness compared to coarse-grained variants, attributed to the distribution of cementite particles which increased work hardening. Similarly, Ning et al. (2013) reported that UFG C45 steel, processed through heat high-pressure torsion, achieved higher tensile strength and ductility than Armco iron, with improvements linked to finer grain structures and dispersed cementite particles. Han & Xu, (2008) investigated the deformation behavior of Fe-32% Ni alloy under multi-axial forging and noted that the flow stress and microstructure depend on deformation temperature, with distinct behaviors at 773K and 1073K . Ohmori et al. (2004) studied severe plastic deformation of 0.16C steel and suggested that grain size is influenced by Zener-Holloman parameters and mechanisms of continuous recrystallization. It is also observed that the MAF process at 420 °C refines Al-Mg composites to submicron grains, significantly enhancing strength and ductility (Wei et al., 2020). Overall, these studies highlight the beneficial effects of ultrafine

grain structures on the mechanical properties of ferrous materials. Few studies about Wear behavior of materials are as follows:

SS 304 having the wide application in surgical and biomedical applications. The ability of 304 steel to withstand the repetitive and often abrasive forces encountered in biomedical devices, such as surgical instruments and implants, is essential to prevent degradation, implant loosening, and the release of potentially harmful wear debris. Therefore, required to check the wear behavior for biomedical application. (Hussain et al. (2015), Naeem et al. (2022)). Abdelgaied et al. (2011) developed a computational wear model for artificial knee joints incorporating a new wear law based on contact area and non-dimensional wear coefficient. Y. Sun et al. (2013), found that surface mechanical attrition-treated AISI 304 steel shows significantly better lubricated wear resistance due to hardened surface layers. As per Archard's wear law high strength material must be wear resistant. But contradictory results were reported by various researchers (Kim et al., 2002, Padap et al., 2010). Hence, it will be interesting to study the wear behavior of the MAC processed stainless steel 304. In view of the above literature, this work lies in exploring the feasibility of using stainless steel 304 as a potential low-cost dental implant material after processing through the MAC technique.

Therefore, the present study aims to develop high-strength stainless steel through warm multiaxial compression (MAC), focusing on its mechanical properties, microstructural evolution, and dry sliding wear behaviour for biomedical applications as a cost-effective alternative to existing implant materials

2.0 EXPERIMENTAL PROCEDURE

2.1 Sample Preparation

Stainless steel 304 having chemical composition (in weight%) as in Table 1 was used for experiments. The samples for MAC were machined into prismatic size of 20×16.33×13.33 mm (refer Figure 1). The proportion of this sample has been specially picked 1.5:1.22:1.0 (Salishchev et al., 1993) for uniform deformation when compressed to compressive strain of 0.4 to longest side of the sample. The samples were annealed at the temperature of 950 ºC for a soaking period of one hour. The samples were allowed to cool inside the furnace after it's shut off. Surface oxidation was observed in the samples after annealing in air atmosphere as shown in Figure 2, which can be attributed to high-temperature exposure in presence of the oxygen present in air. The wear test has been performed on cylindrical pin with 20 mm length and 5 mm diameter as per the ASTM standard G99.

Table 1: Composition of Material SS 304.

Element	C	Mn	P	S	Si	Cr	Ni	N	Fe
Weight %	0.08	2	0.045	0.03	0.75	18-20	8-12	0.1	67-71

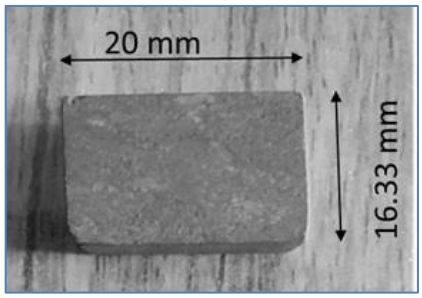

Figure 1: Sample for MAC.

Figure 2: Muffle furnace and samples after Annealing.

2.2 MAC

In MAC, samples were alternately compressed at temperature 500 °C for a soaking time of 50 minutes in X-Y-Z direction through the various passes as depicted schematically in Figure 3a. The load was applied uniaxially on the longest side during each pass with compressive true strain of ε = -0.4, which compresses this side into the shortest one and hence the dimensional ratio is maintained after each compression pass of MAC under the law of mass conservation and within experimental limits. To achieve high strains, multi-axial compression has been performed up to 9 MAC passes on a universal testing machine (Figure 3b). For Avoiding the cracks and achieving uniform deformation, solid lubricant graphite powder was used. It was evenly applied to both top and bottom surfaces of flat die, which reduces the friction between the surfaces of sample and die hence a smooth uniform deformation occurs. After each compression pass, the sample was rapidly quenched into the water to avoid any further microstructural change.

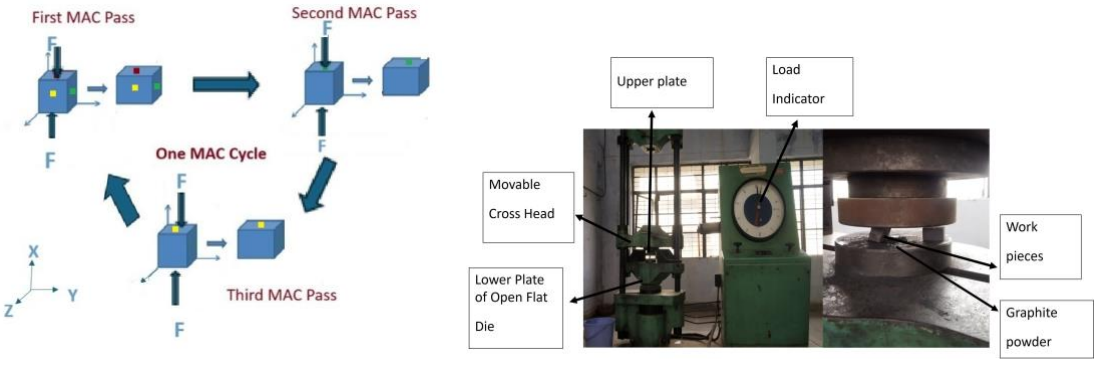

(a) (b)

Figure 3 (a) Schematic diagram of MAC technique (b) Universal testing machine used for MAC

2.3 Microstructural Behavior

Microstructure was observed at the surface perpendicular to last compressive axis. Samples were polished by silicon carbide emery paper of grit size P320, P600, P 1000, P1500 and P2000 respectively for microstructural examination. After paper polishing, samples were fine polished with diamond paste of 0.5 µm size on double disc polishing machine as shown in Figure 4a. In final step, the samples were chemically etched with a solution of 10% HCL + 10% HNO_3 +15%

acetic acid +65% distilled water at room temperature (Figure 4b). Optical microscopy of model Leica DMI 5000M microscopy shown in Figure 5a was used for microstructural characterization.

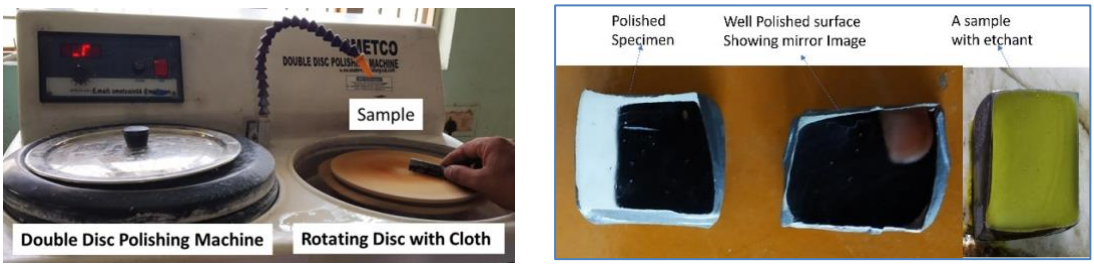

(a) (b)

Figure 4: (a) Double disc polishing machine (b) polished samples

2.4 Vicker's Hardness

Hardness test conducted on Vickers' hardness testing machine VM-50. The surface of workpiece was polished using silicon carbide emery papers of P320, P600, P1000, P1500 and P2000 grit sizes. 5 Kgf load was applied for dwell time of 20 seconds. (Figure 5b)

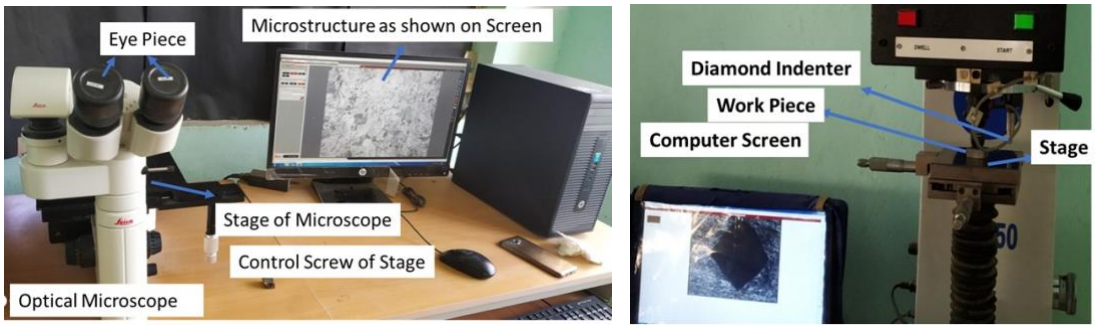

(a) (b)

Figure 5: (a) Optical Microscope (b) Vicker's Hardness testing machine.

2.5 Wear Test

To explore the wear behavior of MAC processed samples as per ASTM G-99, pin-on-disc machine was used (Figure 6 a). The wear samples were machined using wire EDM with a diameter of 5 mm and a height of 20 mm (Figure 6b). Weighing machine with a minimum count of 0.1 mg was used. During the test, apply the load at 40-60 percent relative humidity at 25-30 °C room temperature. The test was conducted against the counter part of the steel disk EN32 with a 65 HRC hardness. The samples were removed after a set sliding time, and weighed to determine weight loss due to wear. The pin's weight loss was evaluated for every 10 minutes of sliding, and then for a complete sliding span of 40 minutes. The test was conducted at the loads of 9.8, 19.6, and 29.4N, and at a constant sliding velocity of 1 m/s. Wear rate were calculated using the following formula:

$$\text{Wear Rate} = \text{Volume loss} / \text{Sliding distance } (mm^3/m)$$

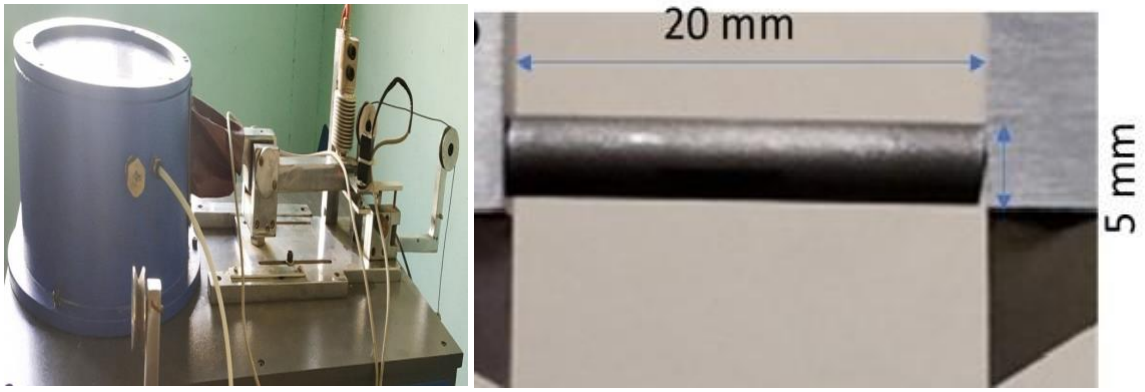

(a) (b)

Figure 6: (a) pin on disc wear test machine. (b) Wear pin for pin on disc wear test.

3.0 RESULTS AND DISCUSSION

3.1 Microstructural Characterization

To find out uniform initial microstructure, annealing of all the samples was performed at temperature 950˚C for 60 minutes. Figure 7a shows the optical micrograph of the annealed samples. It is observed from Figure 7a that grains are mostly equiaxed i.e. uniformly shaped and sized. Grain boundaries are well-defined and relatively straight or gently curved. Multiple grains contain parallel internal lines known as annealing twins, a common feature in FCC austenitic steels. Twins are straight, with sharp interfaces, distinguishing them from deformation twins. No visible signs of slip bands, strain lines, or significant inclusions confirming recrystallized and strain-free condition. Grain size appears moderate to coarse, typically in the range of 40–80 μm. The optical micrograph after 3 MAC passes shown in Figure 7b. it is observed that the original equiaxed austenitic grains have deformed noticeably. Grains appear elongated, flattened, and in many regions show signs of sub-grain formation. High strain has led to distortion of grain boundaries, a signature of heavy warm working. Multiple parallel slip bands are visible inside many grains. These appears due to dislocation motion during plastic deformation. Several grains show prominent deformation twins, typically straight and narrow. Twins are more frequent in austenitic stainless steels under high strain, especially at room temperature due to the FCC structure. Although UFG structure isn't fully developed, fragmented grains and banded contrast zones suggest the onset of Grain subdivision. These are precursors to ultrafine grain formation, especially if further strain or annealing is applied. Grain sizes still appear to be in the tens of microns range (20–40-micron meter, linear intercept method), indicating Partial grain refinement, No full recrystallization yet. This is typical in mid-stage severe plastic deformation (SPD) before ultrafine grain formation is completed. In brief it can be concluded that after three MAC pass grain shape distorted, some elongation and fragmented. Deformation twins in multiple grains were observed. Slip bands prominent, especially in larger grains. Observed substructure suggests pre-UFG stage.

The optical micrograph of six-pass Multi-Axial Compressed (MAC) AISI 304 stainless steel (refer Figure 7c) (true strain ≈ -2.4) reveals several significant microstructural features that

indicate substantial plastic deformation and microstructural refinement due to severe plastic working. It is observed that grains appear significantly smaller and more equiaxed compared to annealed and lower-pass samples (like 3-pass). Average grain size has reduced to ~10–20 μm or smaller, as a result of dynamic recrystallization or subgrain rotation. Grain boundaries are more irregular and denser, indicating intense plastic deformation. Numerous intersecting and parallel slip bands are visible inside many grains. These bands show plastic flow direction and strain accumulation, suggesting active dislocation movement during deformation. Faint, straight, narrow twin lamellae can be seen in some elongated grains. Several large grains appear broken or fragmented, possibly forming subgrains. It indicates dynamic recovery or continuous recrystallization. Darker areas suggest higher strain zones or retained austenite in some grains.

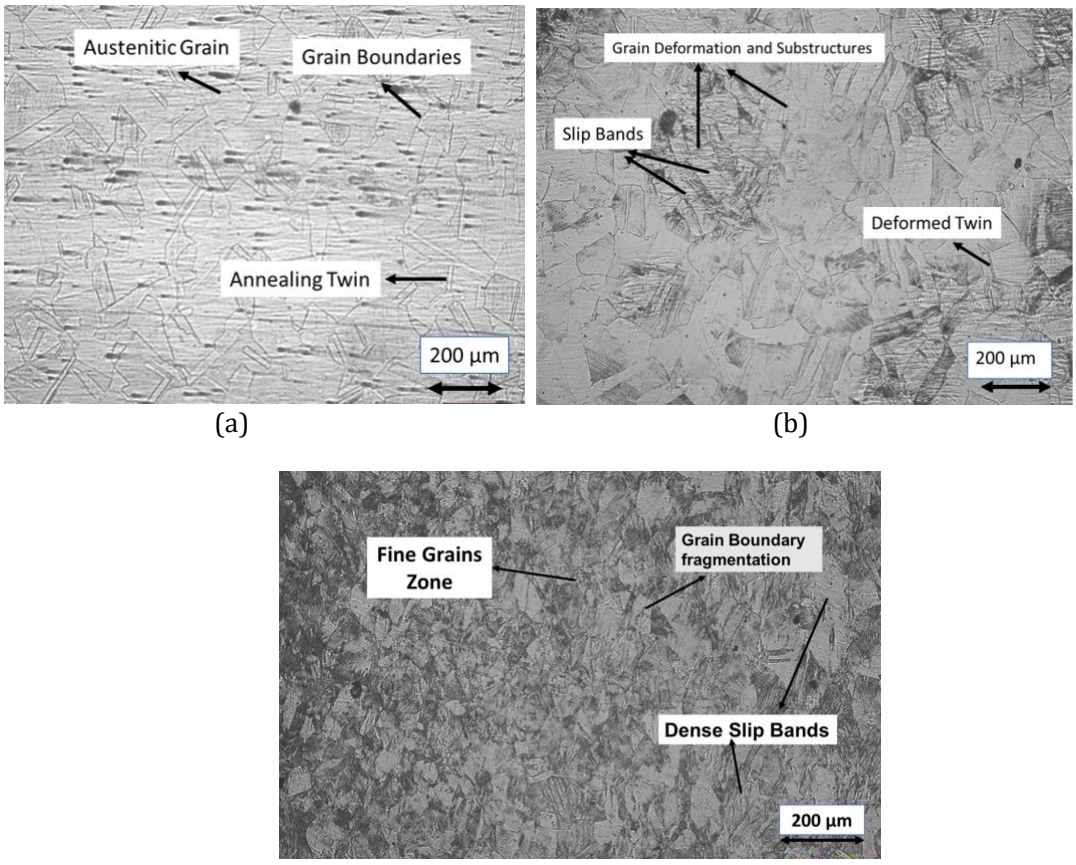

Figure 7: Optical micrograph of (a) Annealed SS 304 sample (b) Three MAC pass sample (c) Six MAC pass sample.

3.2 Vickers Hardness Measurement

Figure 8 shows the variation of hardness values of zero (annealed),1, 2, 3 and 6 MAC passes samples. It is observed that hardness of stainless steel 304 increases from 142.5 VHN to 315 VHN during the test. In six compression passes, the hardness was improved about 2.21 times compared to the annealed sample, which could be the due to strain hardening. It can be corelated with

observed microstructure (Figure 7b &c). The microstructure shows advanced strain hardening, crucial for increasing hardness. Grain refinement and deformation twins contribute to strength via the Hall–Petch effect and twinning-induced plasticity (TWIP). The structure is approaching an UFG or submicron regime. The reduction in grain size increases the number of grain boundaries, which causes the barriers to dislocation motion. This restricted mobility of dislocations enhances resistance to plastic deformation, thereby contributing to the increase in hardness. Hence, grain refinement plays a dominant role in hardness improvement at higher MAC passes, combinedly supported by strain hardening

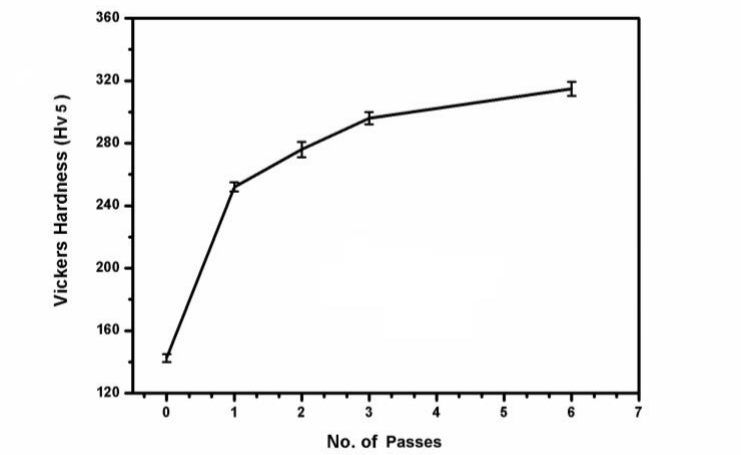

Figure 8: Variation of Vicker's hardness with MAC passes.

3.3 Wear Test Results

The wear test results for annealed and six MAC pass samples at load 9.8N, 19.6N and 29.4N are shown in Figure 9a,9b and 9c. The Figure 9a shows the cumulative volume loss vs cumulative sliding distance. Volume loss increases with sliding distance for all loads, which is typical for dry sliding wear behavior. At lower distances (~600–1200 m), wear trends for all three loads appear comparable or even overlapping, possibly due to the initial oxide formation or running-in effect. At longer distances (>1800 m), volume loss diverges significantly at 29.4 N shows the highest wear, with volume loss at 9.8 N shows the least wear. Similarly, results were observed from Figure 9b six MAC pass sample. But the volume loss for six MAC pass sample is negligibly higher than the annealed sample for all three loads. Figure 9c shows the wear rate of annealed SS 304 and six MAC pass samples which increases with applied load, confirming that, Wear is a stress-assisted thermomechanical process where higher contact pressure promotes more severe material loss (Zum Gahr, 1987). The increasing load leads to greater plastic deformation and possibly delamination wear at high loads. The trend is in line with Archard's wear law, which predicts

wear volume $\propto$ (load × sliding distance) / hardness

Annealed SS 304, having large grain size and soft phase boundaries (refer Figure 7a), which generally offers less resistance to abrasive and adhesive wear. Annealed SS 304 has low hardness (~134) compared to six MAC pass sample (~315) (refer Figure 8) but shows marginally better wear resistance. In six MAC pass sample higher strain induced and grain fragmentation has initiated the multiple crack initiation points which causes the easier and earlier metal loss during the wear test and seems to be the possible reason of decreased wear resistance in spite of

increased hardness. Furthermore, decreased pull off work for six MAC pass sample might also be the reason of marginally decreased wear resistance. It can be further verified from the scanning electron microscope (SEM) image (Figure 10a & 10b) of worn surface of wear test pin

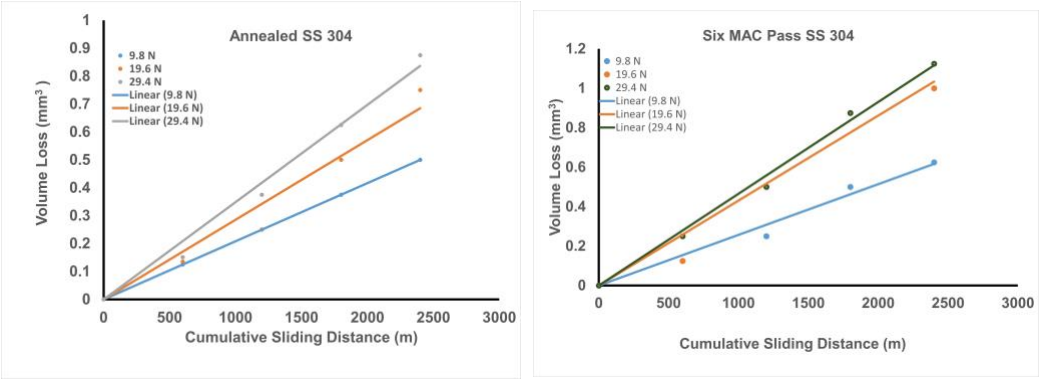

(a) (b)

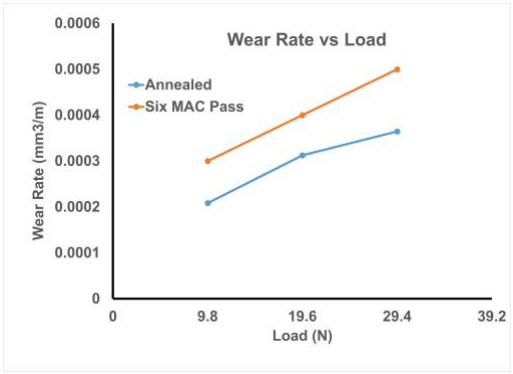

(c)

Figure 9: (a) Volume loss versus sliding distance of annealed samples (b) Volume loss versus sliding distance of six MAC pass sample (c) Wear rate with respect to different loading conditions.

From Figure 10a and 10c, it can be clearly observed that multiple ridges and valleys suggest material removal by micro-cutting action. Smoother regions between grooves indicate plastic flow. Minor evidence of material pile-up and possible adhesive wear spots. Clearly visible parallel grooves and ploughing marks, typical of abrasive wear. The subdued rise in wear rate between 19.6 N and 29.4 N may indicate formation of a mechanically mixed layer / glaze that partially protects the surface, Work hardening of the annealed SS 304 surface during sliding. Transition toward mild oxidative wear stabilizing the wear rate despite higher load. The annealed micrograph showed coarse equiaxed austenitic grains with annealing twins and minimal prior deformation. Such a structure starts comparatively soft higher real contact area develops with load, can deform plastically at asperity junctions and promotes wear debris formation, lacks the strain-hardened subsurface. Wear is likely dominated by adhesive and mild abrasive mechanisms.

Figure 10 b& 10d shows denser and wider wear grooves, more aligned and continuous, suggesting directional sliding wear. higher severe deformation and cutting, possibly due to

increased formation of crack nucleation points due to higher strain induced (ε = -2.4). Micro ploughing with plastic smearing suggests dominant mild abrasive and oxidative wear.

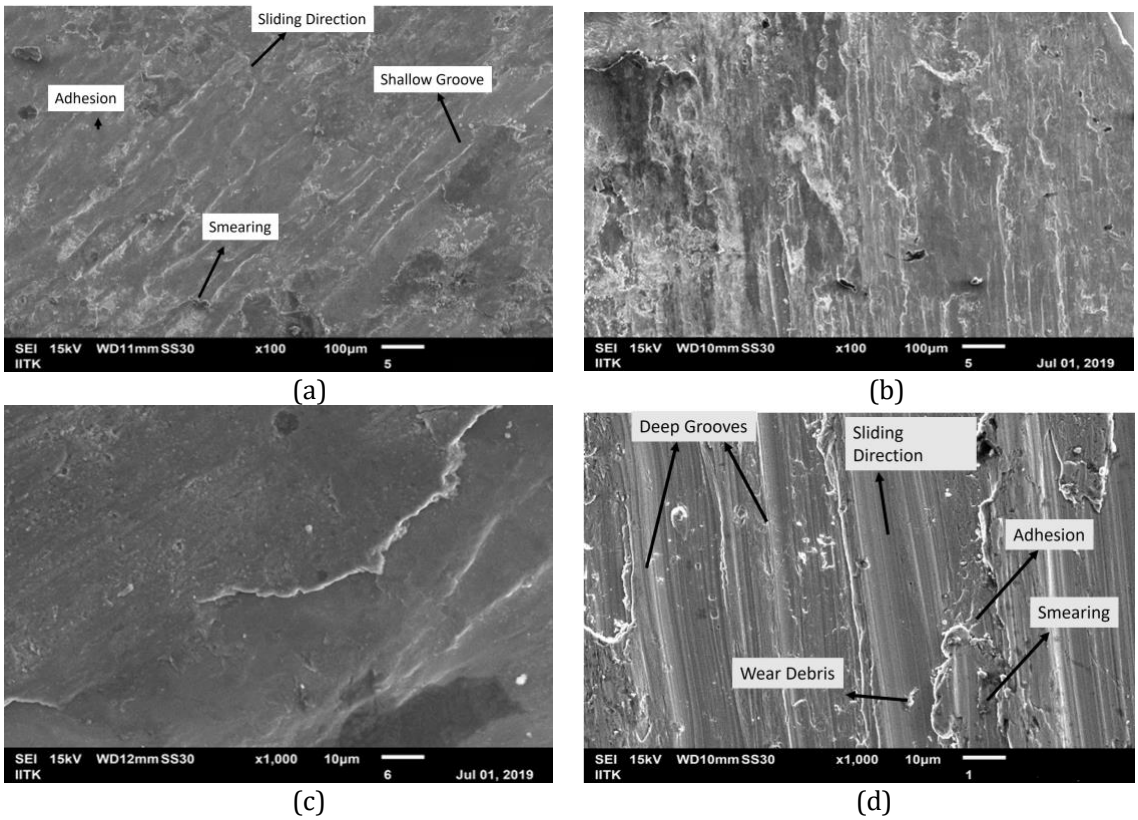

Figure 10: Scanning Electron Microscopic image of wear test pin of (a & c) annealed and (b & d) six MAC pass sample at 19.6N load.

The average coefficient of friction was found to increase with applied load, exhibiting values of 0.31, 0.39, and 0.53 under 9.8 N, 19.6 N, and 29.4 N, respectively. For the six-pass MAC samples, the average coefficient of friction varied as 0.40, 0.50, and 0.52 under the corresponding loads. Overall, the average coefficient of friction increases with load for both conditions. Notably, at lower load, the six-pass MAC samples exhibited a higher coefficient of friction compared to the zero-pass samples. The coefficient of friction is in good agreement with the obtained wear results.

CONCLUSIONS

Stainless steel 304 with 0.08% carbon is multi-axially compressed up to six numbers of strain passes. Mechanical, wear and micro structural behavior of the MAC steel was studied. It was observed that hardness and wear properties of stainless steel 304 were strongly influenced by the process of MAC. However, the observed wear resistance of MAC processed SS 304 is comparable with annealed sample. The following conclusions has been drawn.

(a) Hardness value for annealed sample is 134 while 315 VHN for six MAC pass. Increased hardness about 70% after six MAC pass sample is attributed to strain hardening as well as grain refinement observed in six MAC pass samples.
(b) Observation of the optical micrograph after third MAC pass showed the development of sub grains which get dense after six MAC passes. This is due to the heavy strain induced during MAC and complex stress reversal during the process. Grains also refined from 80 μm in annealed sample to 10 μm in six MAC pass samples
(c) The cumulative volume loss increases with increased in load and cumulative sliding distance for annealed and MAC processed samples.
(d) Wear rate is found to be marginally higher for six MAC pass at room temperature than annealed sample. This might be due to the high crack nucleation points generated at higher strain induced of the samples deformed up to six MAC passes.
(e) Observed wear mechanism in annealed and six MAC pass sample were corelated with worn surfaces of wear pin and microstructure.

REFERENCES

Abdelgaied, A., Fisher, J., & Jennings, L. M. (2011). Computational wear prediction of artificial knee joints based on a new wear law and formulation. Journal of Biomechanics, 44(6), 1108–1116.
Aravindh, G., Preetham Kumar, G. V., & Udaya Bhat, K. (2025). Enhancement of mechanical and tribological properties of Sm-modified Al5083 alloy through multiaxial forging. Results in Engineering, 27, 105954.
Bhadeshia, H., & Honeycombe, R. (2017). Steels: Microstructure and Properties (4th ed.). Butterworth-Heinemann, an imprint of Elsevier.
Bhushan, B. (2013). Introduction to Tribology (2nd ed.). Wiley.
Blau, P. J. (2001). The significance and use of the wear coefficient. Tribology International, 34(9), 585–591.
Callister, W. D., & Rethwisch, D. G. (2014). Materials Science and Engineering: An Introduction (9th ed.). Wiley.
Han, B., & Xu, Z. (2006). Grain refinement mechanism of Fe–32Ni alloys during multiaxial forging. Materials Science and Technology, 22(11), 1359–1363.
Han, B., & Xu, Z. (2008). Grain refinement under multi-axial forging in Fe–32%Ni alloy. Journal of Alloys and Compounds, 457, 279–285.
Hussein, M. A., Mohammed, A. S., & Al-Aqeeli, N. (2015). Wear characteristics of metallic biomaterials: A review. Materials, 8, 2749–2768.
Kim, Y. S., Lee, T., Park, K. T., Kim, W. J., & Shin, D. H. (2002). TMS (UFG Materials II, Proceedings of a Symposium, TMS Annual Meeting).
Ma, E. (2003). Instabilities and ductility of nanocrystalline and ultrafine-grained metals. Scripta Materialia, 49(7), 663–668.
Meyers, M. A., & Chawla, K. K. (2008). Mechanical Behavior of Materials (2nd ed.). Cambridge University Press.
Naeem, M., Awan, S., Shafiq, M., Raza, H. A., Iqbal, J., Díaz-Guillén, J. C., Sousa, R. R. M., Jelani, M., & Abrar, M. (2022). Wear and corrosion studies of duplex surface-treated AISI-304 steel by a combination of cathodic cage plasma nitriding and PVD-TiN coating. Ceramics International, 48(15), 21473–21482.

Ning, J., Courtois-Manara, E., Kurmanaeva, L., Ganeev, A. V., Valiev, R. Z., Kübel, C., & Ivanisenko, Y. (2013). Tensile properties and work hardening behaviors of ultrafine grained carbon steel and pure iron processed by warm high pressure torsion. Materials Science and Engineering: A, 581, 8–15.

Ohmori, A., Torizuka, S., & Nagai, K. (2004). Strain-hardening due to dispersed cementite for low carbon ultrafine-grained steels. ISIJ International, 44(6), 1063–1071.

Padap, A. K., Chaudhari, G. P., Nath, S. K., & Pancholi, V. (2009). Ultrafine-grained steel fabricated using warm multiaxial forging: Microstructure and mechanical properties. Materials Science and Engineering: A, 527(1–2), 110–117.

Padap, A. K., Chaudhari, G. P., Pancholi, V., & Nath, S. K. (2010). Warm multiaxial forging of AISI 1016 steel. Materials & Design, 31(8), 3816–3824.

Padap, A. K., Chaudhari, G. P., & Nath, S. K. (2010). Mechanical and dry sliding wear behavior of ultrafine-grained AISI 1024 steel processed using multiaxial forging. Journal of Materials Science, 45, 4837–4845.

Rabinowicz, E. (2013). Friction and Wear of Materials (2nd ed.). Wiley-Interscience Publication, John Wiley & Sons, Inc.

Salishchev, G. A., Valiakhmetov, O. R., & Galeyev, R. M. (1993). Formation of submicrocrystalline structure in the titanium alloy VT8 and its influence on mechanical properties. Journal of Materials Science, 28(11), 2898–2902.

Sauvage, X., Wilde, G., Divinski, S. V., Horita, Z., & Valiev, R. Z. (2008). Nanostructure and properties of a Cu–Cr composite processed by severe plastic deformation. Scripta Materialia, 58(12), 1125–1128.

Song, R., Ponge, D., & Raabe, D. (2005). Mechanical properties of an ultrafine grained C–Mn steel processed by warm deformation and annealing. Acta Materialia, 53(18), 4881–4892.

Suh, N. P. (1973). The delamination theory of wear. Wear, 25(1), 111–124.

Sun, Y. (2013). Sliding wear behaviour of surface mechanical attrition-treated AISI 304 stainless steel. Tribology International, 57, 67–75.

Tsuji, N., Ito, Y., Saito, Y., & Minamino, Y. (2002). Strength and ductility of ultrafine grained aluminum and iron produced by ARB and annealing. Scripta Materialia, 47(12), 893–899.

Tsuji, N., Saito, Y., Utsunomiya, H., & Tanigawa, S. (1999). Ultra-fine grained bulk steel produced by accumulative roll-bonding (ARB) process. Scripta Materialia, 40(7), 795–800.

Valiev, R. Z., Islamgaliev, R. K., & Alexandrov, I. V. (2000). Bulk nanostructured materials from severe plastic deformation. Progress in Materials Science, 45(2), 103–189.

Valiev, R. Z., Islamgaliev, R. K., Alexandrov, I. V., & Langdon, T. G. (1999). Structure and mechanical properties of ultrafine-grained metals. Materials Science and Engineering: A, 234–236, 59–66.

Vinogradov, A., & Hashimoto, S. (2001). Multiscale phenomena in ultrafine-grained metals produced by SPD. Materials Transactions, 42(1), 74–84.

Wei, J., Jiang, S., Chen, Z., & Liu, C. (2020). Increasing strength and ductility of a Mg–9Al alloy by dynamic precipitation assisted grain refinement during multi-directional forging. Materials Science and Engineering: A, 780, 139192.

Xu, C., Horita, Z., & Langdon, T. G. (2007). The evolution of homogeneity in processing by high-pressure torsion. Acta Materialia, 55(1), 203–212.

Zhilyaev, A. P., & Langdon, T. G. (2008). Using high-pressure torsion for metal processing: Fundamentals and applications. Progress in Materials Science, 53(6), 893–979.

Zum Gahr, K.-H. (1987). Microstructure and wear of materials. Tribology Series 10. Elsevier.